Cluster-Size Distribution of Cross-Linked Polymer Chains across the Gelation Threshold

Tomohisa Norisuye, Masanao Takeda, and Mitsuhiro Shibayama*

Department of Polymer Science and Engineering, Kyoto Institute of Technology, Matsugasaki, Sakyo-ku, Kyoto 606-8585, Japan

Received February 6, 1998; Revised Manuscript Received April 25, 1998

ABSTRACT: The evolution of cross-linked polymer chain clusters in a solvent from a monomer solution has been investigated by dynamic light scattering. The characteristic decay time distribution, $P(\Gamma^{-1})$, of the gelling system has been examined as a function of the initial monomer concentration, C, where Γ^{-1} and Γ are the characteristic decay time and the decay rate, respectively. When C is lower than the chain overlap concentration C^*, $P(\Gamma^{-1})$ is dominated by a single peak related to clusters having a hydrodynamic radius of R_H. However, for $C \approx C^*$, $P(\Gamma^{-1})$ becomes broader, having a tail toward a larger value of Γ^{-1}. This indicates a formation of an assemble of clusters with a broad size distribution. On the other hand, for $C > C^*$, $P(\Gamma^{-1})$ becomes narrow and unimodal, which results from scattering by an infinite network and corresponds to the so-called gel mode scattering. This behavior is very different from that for the corresponding polymer solutions with the same concentrations. On the basis of these results, the time evolution of the dynamics of polymer gels will be discussed.

Introduction

Kinetics of gelation is an attractive research problem in order to clarify the gel structure and the chemistry of gelation. For example, in the industry, determination of the gelation threshold is an important issue to control the mechanical and rheological properties of a gelling system. The light scattering technique is one of the most suitable means to study a gelation process without disturbing the gelling system.[1,2] Regarding the functional form of the intensity time correlation function, $g^{(2)}(\tau)$, Tanaka et al.[3] have shown that $g^{(2)}(\tau)$ can be expressed with a single exponential function with the decay time, τ, for chemically cross-linked poly(acrylamide) gels, even though the chain length between neighboring cross-links is widely distributed. This is due to the cooperative nature of polymer networks in the solvent. That is, any part of polymer chains cannot move freely by itself because it is connected via cross-links. However, it has still been an open question whether such single-exponential behavior in $g^{(2)}(\tau)$ is universal for any kind of gels or when it is attained during the gelation process. In the literature, there are a large number of studies that report non-single exponential behavior for $g^{(2)}(\tau)$. For example, Munch et al. obtained double-exponentially decaying correlation functions for a system of styrene with divinylbenzene undergoing gelation by radical copolymerization.[4] The decay rates of the fast and slow modes were very different, and they interpreted that the fast and slow modes represented cooperative concentration fluctuations and diffusions of aggregates, respectively. Adam et al. reported that $g^{(2)}(\tau)$ had a stretched exponential form for a gelling system with concentrations lower than a particular concentration (the polymer volume fraction of $\phi \approx 0.07$) and it became a power law function above this concentration.[5] Martin et al.[1,6,7] observed a similar behavior, i.e., a stretched exponential decay, for a reaction bath of silica gels and epoxy networks. They also reported that $g^{(2)}(\tau)$ becomes a power law function at the gelation threshold and remains a power law form even in the gel regime.[2] Shibayama reported that a double exponential function or a stretched exponential function is a more suitable function for a weakly charged gel near the volume phase transition temperature.[8] By considering these experimental results, it is of particular importance to examine the validity and the extent of applicability of a single exponential fit for $g^{(2)}(\tau)$ in studying various types of polymer gels prepared under various conditions. We employ here a distribution function, $P(\Gamma^{-1})$, for the characteristic decay time Γ^{-1}, as a tool for evaluation of the applicability of the single exponential fit for gels, and investigate the dynamics of a gelling system. The gelation mechanism will also be discussed on the basis of the time evolution of $P(\Gamma^{-1})$ for gels having different C's.

Theoretical Background

In the case of polymer gels, it was shown by Tanaka et al.[3] that the intensity time correlation function, $g^{(2)}(\tau)$, for polymer networks in a solvent can be given by a single exponential function, as follows,

$$g^{(2)}(\tau) - 1 = \sigma_I^2 \exp[-2\Gamma_0\tau] \quad (1)$$

where σ_I^2 is the initial amplitude of the correlation function and Γ_0 is the characteristic rate for the cooperative diffusion of the network in the gel. Γ_0 is related to the cooperative diffusion coefficient, D, with the following equation,

$$\Gamma_0 = Dq^2 \quad (2)$$

However, near the gelation threshold, it is expected that the decay rate, Γ, has a wide distribution. As a result, $g^{(2)}(\tau)$ becomes an nonexponential function. Instead of introducing a distribution of Γ, a stretched exponential or a power law function, having the following forms, is commonly used to analyze $g^{(2)}(\tau)$:

* To whom correspondence should be addressed.

S0024-9297(98)00182-X CCC: $15.00
Published on Web 07/24/1998

$$g^{(2)}(\tau) - 1 = \sigma_I^2 \exp[-(\Gamma_{st}\tau)^{\beta}] \quad \text{(stretched exponential)} \quad (3)$$

$$g^{(2)}(\tau) - 1 \sim (\Gamma_{pw}\tau)^{-\alpha} \quad \text{(power law)} \quad (4)$$

where (β, Γ_{st}) and (α, Γ_{pw}) are (the exponent, the characteristic decay rate) defined by eqs 3 and 4, respectively. Although the latter is ascribed to the dynamic scaling of the critical exponents,[9] the former is purely an empirical expression. In both cases, analyses are carried out by fitting the observed $g^{(2)}(\tau)$ with the theoretical ones given by eq 3 or 4.

However, it would be more relevant if one can directly evaluate the distribution of Γ. Such an analysis can be conducted by taking the inverse Laplace transform (ILT) of $g^{(2)}(\tau)$. Among many algorithms, the CONTIN method (the constrained regularization method) is justified to be one of the most faithful methods to represent the distribution of Γ, i.e., the characteristic decay rate distribution function, $G(\Gamma)$.[10−12] $G(\Gamma)$ is defined by the first-order electric-field time correlation function $g^{(1)}(\tau)$ for a polydisperse system:

$$g^{(1)}(\tau) \equiv \frac{\langle f(t)\, f^*(t+\tau)\rangle}{|f(t)|^2} = \int_0^\infty G(\Gamma) \exp[-\Gamma\tau]\, d\Gamma \quad (5)$$

where $f(t)$ and $f^*(t)$ are the electric fields of the scattered light at time t and its complex conjugate, respectively. Instead of eq 5, the second-order correlation function, i.e., the intensity time correlation function, $g^{(2)}(\tau)$, is more frequently used in order to obtain $G(\Gamma)$ by using the following equation:

$$g^{(2)}(\tau) - 1 = [\int_0^\infty G(\Gamma) \exp(-\Gamma\tau)\, d\Gamma]^2 \quad (6)$$

Equation 6 is derived by using the Siegert relation,

$$g^{(2)}(\tau) = 1 + |g^{(1)}(\tau)|^2 \quad (7)$$

Therefore, it should be noted that eq 6 is valid only for ergodic media. In the case of nonergodic media, such as polymer gels, $g^{(2)}(\tau)$ has both homodyne and heterodyne components, as written by[13]

$$g^{(2)}(\tau) - 1 = X^2\{g^{(1)}(\tau)\}^2 + 2X(1 - X)g^{(1)}(\tau) \quad (8)$$

X is the ratio of the intensites of the fluctuating component $\langle I_F\rangle_T$ to the total intensity $\langle I\rangle_T$ as is given by

$$X = \frac{\langle I_F\rangle_T}{\langle I\rangle_T} \quad (9)$$

where $\langle ...\rangle_T$ denotes time average. In this case, $G(\Gamma)$ defined by eq 5 is slightly different from that defined by eq 6. For example, $g^{(1)}(\tau)$ and $g^{(2)}(\tau)$ give the characteristic decay rates of Γ_0 and $2\Gamma_0$, respectively, provided that $g^{(1)}(\tau)$ is given by a single exponential function. This difference, by a factor of 2, does not make a significant effect in evaluating $G(\Gamma)$. Therefore, we do not discuss this issue further and simply analyze $G(\Gamma)$ obtained by eq 5 both for linear and cross-linked polymer chains in a solvent.

The advantage to using the ILT method is that the distribution of the characteristic decay rate can be visualized as a function of Γ. For example, when $G(\Gamma) = \sigma_I^2\delta(\Gamma - \Gamma_0)$, eq 6 is reduced to eq 1, and a single exponential behavior is recovered, where $\delta(x)$ is the Dirac delta function and Γ_0 is the characteristic decay rate of the system. It should also be noted that we use a characteristic decay time distribution function, $P(\Gamma^{-1}) \equiv G(\Gamma)$, instead of $G(\Gamma)$. This is because $P(\Gamma^{-1})$ is more commonly used to represent the distribution of the characteristic decay time, Γ^{-1}, and it provides information of a kind of "spectrum" of $g^{(2)}(\tau)$.

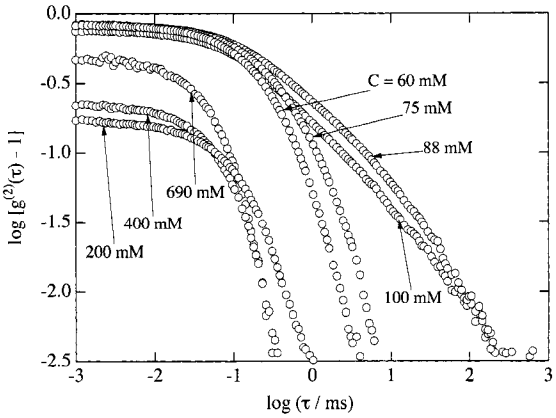

Figure 1. Double logarithmic plot of the intensity-time correlation function, $g^{(2)}(\tau) - 1$, for cross-linked NIPA polymer chains in a solvent with various C's.

Experimental Section

Sample. A series of cross-linked poly(*N*-isopropylacrylamide) (NIPA) were prepared by redox polymerization in aqueous media. The monomer concentration of NIPA at preparation, C, was varied from 48 to 60, 75, 88, 100, 200, 400, and 690 mM, while the cross-linker concentration (*N*,*N*′-methylenebis(acrylamide); BIS) and the initiator concentration (ammonium persulfate) were fixed to be 8.62 mM and 1.75 mM, respectively. These monomers and reagents were dissolved in distilled water, filtered with a 0.2 μm filter, and then degassed. After the mixture solutions were chilled in a refrigerator for about 30 min, 8 mM of tetramethylethylenediamine was added and the reaction was initiated. The polymerization/cross-linking was conducted in a 5-mm quartz test tube at 20 °C. A series of corresponding NIPA linear polymer solutions having the same monomer concentrations were also prepared with the same manner without adding BIS.

Dynamic Light Scattering. Dynamic light scattering (DLS) measurements were carried out on a DLS/SLS-5000 compact goniometer, ALV, Langen, coupled with an ALV photon correlator. A 35-mW helium−neon laser (the wavelength in vacuum; λ = 632.8 nm) was used as the incident beam. In order to obtain ensemble average, the intensity time correlation function, $g^{(2)}(\tau)$, was obtained at 100 different sample positions. All the measurements were carried out at 20 °C. The acquisition time for each run was 5 min. The characteristic decay time distribution function $P(\Gamma^{-1})$, was obtained from $g^{(2)}(\tau)$ with an inverse Laplace transform program (a constrained regularization program, CONTIN provided by ALV).[14]

Results and Discussion

1. Cross-Linked Polymer Chains in a Solvent. Figure 1 shows double logarithmic plots of the intensity time correlation function, $\log[g^{(2)}(\tau) - 1]$, for cross-linked NIPA polymer chains in a solvent having various C's. For $C \le 75$ mM, $g^{(2)}(\tau)$ has a characteristic decay at $\tau \approx 10$ ms. For C = 88 and 100 mM, $g^{(2)}(\tau)$ has a long tail at the larger value of τ. This corresponds to the gelation threshold at which the connectivity correlation diverges, as will be discussed later. However, even at these concentrations, $g^{(2)}(\tau)$ cannot be described by a power law type function, which is different from the results

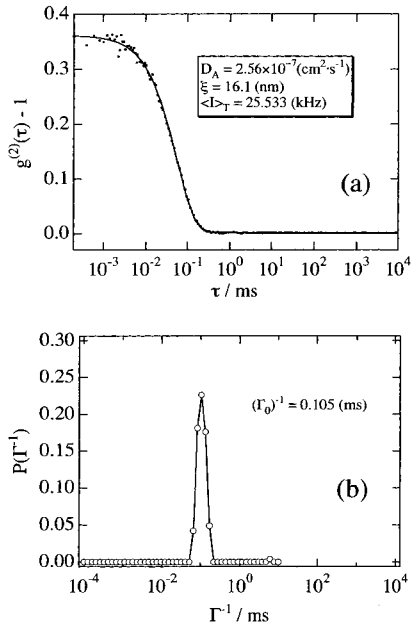

Figure 2. (a) Intensity time correlation function, $g^{(2)}(\tau)$, and (b) the characteristic decay time distribution function, $P(\Gamma^{-1})$, for NIPA gels with $C = 690$ mM.

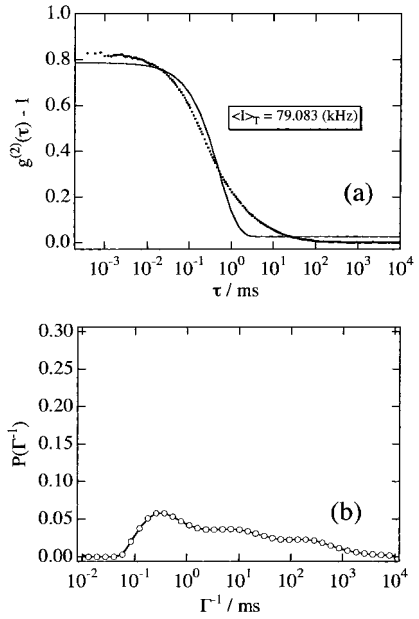

Figure 3. (a) Intensity time correlation function, $g^{(2)}(\tau)$ and (b) the characteristic decay time distribution function, $P(\Gamma^{-1})$ for a cross-linked NIPA finite cluster solution with $C = 88$ mM.

reported in the literature.[1,2,6] For $C \geq 200$ mM, $g^{(2)}(\tau)$ recovers a behavior similar to the case of $C \leq 75$ mM. However, there are two characteristic features in $g^{(2)}(\tau)$ for $C \geq 200$ mM; (i) the characteristic decay time being much smaller, i.e., $\tau \approx 10^{-1}$ ms, and (ii) the value of $g^{(2)}(\tau\rightarrow0)$ being much lower than unity. The latter indicates that the system becomes nonergodic and $g^{(2)}(\tau\rightarrow0)$ $(=\sigma_I^2)$ depends on the sample position.[15] The behavior of $g^{(2)}(\tau)$ for $C > 200$ mM is also very different from that obtained by Martin et al., who obtained a power law functional form even for a well-developed gel.[2] Therefore, it is clear that such a power law function analysis is not relevant for gels studied in this work, e.g., a chemically cross-linked gel in a reactor batch prepared by radical polymerization from a vinyl monomer solution. In order to investigate the change in $g^{(2)}(\tau)$ with C more quantitatively, we examine the characteristic decay time distribution function, $P(\Gamma^{-1})$, as a function of C.

Figure 2 shows (a) the intensity time correlation function, $g^{(2)}(\tau)$, and (b) the characteristic decay time distribution function, $P(\Gamma^{-1})$, for NIPA gels with $C =$ 690 mM. The solid line indicates the fitted curve with a single exponential function (eq 1) with an apparent diffusion coefficient, D_A $(\equiv\Gamma_0/q^2)$. As shown in Figure 2a, $g^{(2)}(\tau)$ for the NIPA gel is successfully represented by a single exponential function. Figure 2b shows that $P(\Gamma^{-1})$ is sharp and unimodal, supporting the validity of a single-exponential-function analysis. Therefore, Figure 2a,b clearly indicates that $g^{(2)}(\tau)$ for gels, like NIPA gels, is described by a single exponential function, as predicted by Tanaka et al.[3] It should be noted, however, that there are many types of gels, like tetramethoxysilane gels, of which $g^{(2)}(\tau)$ cannot be described by eq 1.[2]

If the monomer concentration, C, is lowered below the critical concentration, C^*, at which chain overlap takes place, infinite networks cannot be formed at all but finite clusters of cross-linked polymer chains may be floated in the solvent. The C^* for linear poly-NIPA aqueous solutions, prepared in the same manner and observed at 25 °C, was estimated to be ca. 110 mM by light scattering and viscometry.[16] Therefore, the broad distribution of $P(\Gamma^{-1})$ is expected for polymer solutions prepared around this concentration. Figure 3 shows (a) $g^{(2)}(\tau)$ (b) $P(\Gamma^{-1})$ for a poly-NIPA finite cluster solution with $C = 88$ mM. A noticeable deviation from a single exponential function (solid line) is clearly seen in Figure 3a. Accordingly, as shown in Figure 3b, $P(\Gamma^{-1})$ now has a broad tail at larger value of Γ^{-1}, indicating the presence of a broad distribution of clusters. These figures show that $P(\Gamma^{-1})$ for solutions having cross-linked polymer clusters of finite sizes cannot be described with a single exponential function.

Figure 4 shows a series of $P(\Gamma^{-1})$'s for NIPA gels having various initial monomer concentrations. In order to demonstrate the nonergodic nature of polymer gels ($C \geq 200$ mM), 10 $P(\Gamma^{-1})$'s obtained at 10 different sample positions are shown for each sample with different C's. Roughly speaking, $P(\Gamma^{-1})$'s can be superimposed with each other for $C < 200$ mM. By a careful observation of $P(\Gamma^{-1})$'s for $C \geq 200$ mM, one finds that the peak position has a distribution within a limited range of Γ^{-1}. This is due to the nonergodic nature of the gels.[15] In addition, as demonstrated in Figure 2, $g^{(2)}(\tau)$ for gels with $C \geq 200$ mM can be represented by a single exponential function. However, for $C \leq 88$ mM, a single exponential fit does not work, as shown in Figure 3 for the case of $C = 88$ mM. In these cases, the dynamics is governed by a motion of "finite" clusters of poly-NIPA with the hydrodynamic radius, R_H, of

$$R_H = \frac{kT}{6\pi\eta D_A} \approx \frac{kTq^2}{6\pi\eta\Gamma} \tag{10}$$

where η is the solvent viscosity. For $C = 60$ mM, $P(\Gamma^{-1})$ is unimodal and a representative value of R_H can be estimated to be 80 nm by letting $\Gamma = \Gamma_0$, i.e., the value of Γ which gives the maximum in $P(\Gamma^{-1})$. This corresponds to a typical size of polymer chain clusters dispersed in the solvent. On the other hand, for $C \geq$ 200 mM, the single peak in $P(\Gamma^{-1})$ represents the

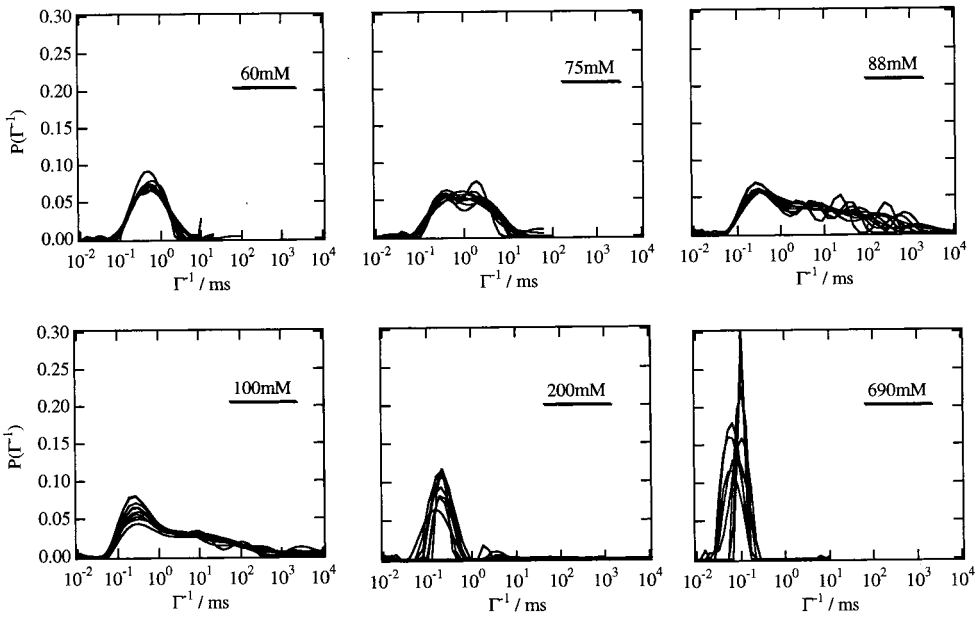

Figure 4. Characteristic decay time distribution functions, $P(\Gamma^{-1})$, of cross-linked NIPA polymer solutions (for $C < C^*$) and of NIPA gels (for $C > C^*$). Due to nonergodicity, 100 $P(\Gamma^{-1})$'s were measured at different sample positions for each concentration and 10 $P(\Gamma^{-1})$'s were shown. For $C > 200$ mM, a monodisperse distribution of $P(\Gamma^{-1})$ is obtained, indicating that the system is in the gel mode. For $88 \leq C \leq 100$ mM, the distribution has a tail at larger Γ^{-1}. This corresponds to the presence of large finite clusters of cross-linked poly-NIPA chains.

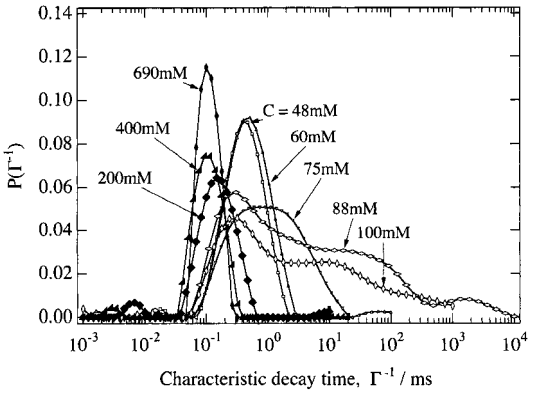

Figure 5. Monomer concentration dependence of representative $P(\Gamma^{-1})$ for cross-linked poly-NIPA chains with $C = 48$, 60, 75, 88, 100, 200, 400, and 690 mM.

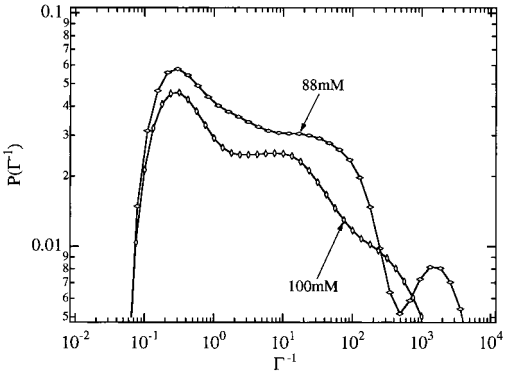

Figure 6. Double logarithmic plot of $P(\Gamma^{-1})$ vs Γ^{-1} for NIPA cross-linked polymer chains in a solvent at $C = 88$ and 100 mM.

cooperative diffusion of the polymer network with the correlation length, ξ, as follows:[9]

$$\xi \approx \frac{kT}{6\pi\eta D_A} = \frac{kTq^2}{6\pi\eta\Gamma_0} \tag{11}$$

where D_A is the apparent diffusion coefficient. Here, since polymer chains are heavily overlapped, only cooperative-concentration fluctuations in the medium of polymer matrix are allowed. For instance, ξ's are estimated to be 10 and 14 nm for the 690 mM NIPA gel and the corresponding polymer solution, respectively, which are much smaller than R_H for the 60 mM poly-NIPA cluster solution. It should be noted here that D_A depends on the position of the sample due to nonergodicity (more rigorously speaking, restricted ergodicity) of the network.[13,17,18] However, it is known that D_A has both a lower and upper limit, i.e., $D/2 \leq D_A \leq D$, where D is the cooperative diffusion coefficient of the system.[13] Thus, the dynamics of the gels is uniquely characterized by D.

In the intermediate concentration regime (i.e., $88 \leq C \leq 100$ mM in this particular case), $g^{(2)}(\tau)$ cannot be fitted with a single exponential function, as shown in Figure 3a, and a distribution analysis is required. This is the regime where some finite clusters become an infinite cluster by slightly increasing C at preparation. In other words, this is the regime of the gelation threshold. The chain overlap concentration, C^*, can be obtained from the intrinsic viscosity, $[\eta]$, via,

$$C^* = \frac{3 \times 6^{3/2}\Phi}{4\pi N_A[\eta]} \tag{12}$$

where N_A is the Avogadro's number and Φ is the universal constant. The value of Φ is known to be 2.1×10^{23} for polydisperse dilute polymer solutions.[19] In our previous paper, the intrinsic viscosity, $[\eta]$, for a poly-NIPA aqueous solution with $C = 88$ mM was estimated to be 96.6 $cm^3\ g^{-1}$ at 25 °C, which readily leads to $C^* \approx$ 110 mM.[16] Therefore, the lowest concentration of NIPA monomers to form an infinite cluster is estimated to be around 110 mM for poly-NIPA aqueous solutions prepared by redox polymerization at 20 °C. By comparing both results obtained by viscometry and DLS, one can

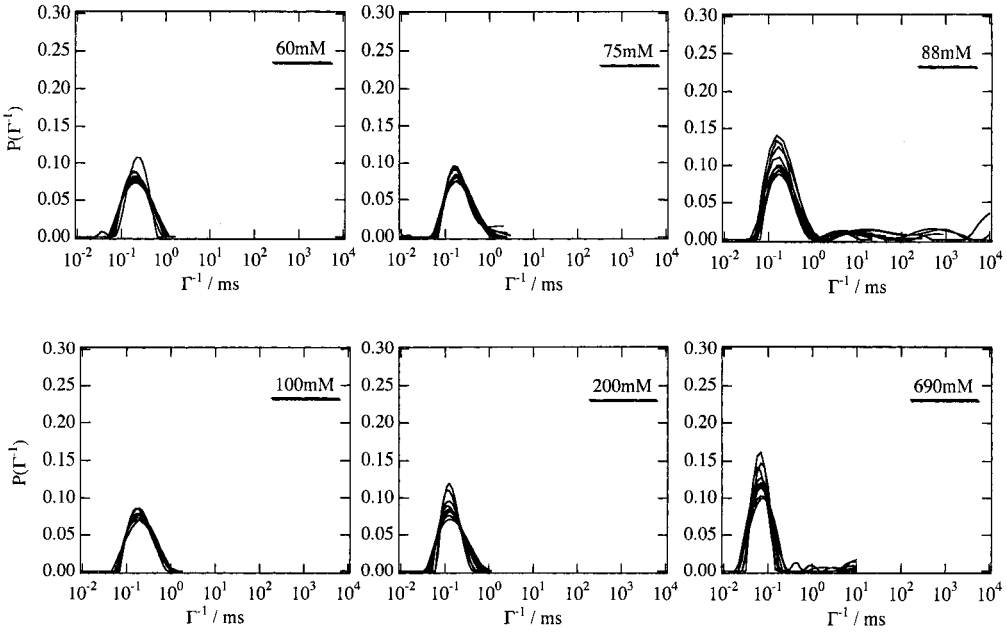

Figure 7. Series of distribution functions of the characteristics decay time, $P(\Gamma^{-1})$, for NIPA linear polymer chain solutions having the same concentrations as the NIPA gels.

conclude that the gelation threshold can be determined by the analysis of $P(\Gamma^{-1})$ for cross-linked polymer chains in a solvent prepared with various C's.

Figure 5 summarizes the monomer concentration dependence of representative $P(\Gamma^{-1})$'s for cross-linked NIPA polymer clusters with $C = 48$, 60, 75, 88, 100, 200, 400, and 690 mM. This figure clearly shows the variation of the shape of $P(\Gamma^{-1})$ as well as the peak position in $P(\Gamma^{-1})$. $P(\Gamma^{-1})$ is unimodal for $C \leq 60$ mM but becomes broader for $C \geq 75$ mM. Note that the peak position moves toward a larger value of Γ^{-1} with C. A very broad distribution is observed at the concentration regime between 88 and 100 mM where the gelation threshold is located. For $C \geq 200$ mM, a unimodal distribution is recovered, which corresponds to the so-called gel mode scattering, i.e., a single exponential behavior in $g^{(2)}(\tau)$.

If $g^{(2)}(\tau)$ is described by a power law function, $P(\Gamma^{-1})$ is also expected to be a power law function because of the nature of Laplace transform. Figure 6 shows double logarithmic plots of $P(\Gamma^{-1})$ for $C = 88$ and 100 mM. This figure clearly shows that $P(\Gamma^{-1})$ cannot be approximated by a power law function, at least for polymer gels studied in this work.

2. Linear Chain Clusters in a Solvent. Figure 7 shows a series of distribution functions of the characteristic decay time, $P(\Gamma^{-1})$, for NIPA linear polymer solutions having various monomer concentrations. In contrast to Figure 3, it is clear that no significant peak broadening in $P(\Gamma^{-1})$ is observed for the NIPA polymer solutions at $88 \leq C \leq 100$ mM. Though a slight broadening is observed for $C = 88$ mM, it is much narrower than the case of the gels. This indicates that the perimeters of NIPA polymer chains gradually merge to each other with increasing C. The wide distribution in $P(\Gamma^{-1})$ for cross-liked chains at $C = 88$ and 100 mM seems to be a result of the cascade nature of cross-linking. That is, the mass increases by a factor of 2 by each coupling. It is easily expected that the mass of well-grown-finite clusters can be increased in a cascade fashion by coupling them with a small number of cross-links. This may be why $P(\Gamma^{-1})$ for the gels has a long tail at Γ^{-1}. Thermal fluctuations in the linear polymer chain system may promote interchain mixing. It is important to estimate the molecular weight of NIPA polymer chains. We estimated the viscosity-average molecular weight, M_v, for the poly-NIPA solution at $C = 88$ mM to be about 6.0×10^5 from the data of $[\eta]$, via the so-called Mark−Houwink−Sakurada equation,

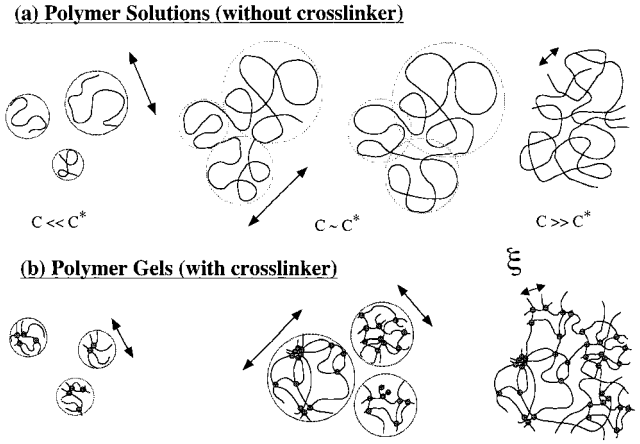

Figure 8. Schematic illustration showing the monomer concentration depedence of $P(\Gamma^{-1})$ for (a) linear polymer chain solutions and (b) cross-linked polymers in a solvent.

$$[\eta] = KM^a \tag{13}$$

where the values of K and a were chosen to be the reported values by Kubota et al., i.e., $K = 0.11$ and $a = 0.51$.[20]

3. Model of Polymer Chain Clusters. The origin of the clear difference in the concentration dependence of $P(\Gamma^{-1})$'s between the two systems with and without cross-linkers may be explained with Figure 8. In the case of polymer solutions (in the absence of cross-linkers), the envelope of individual polymer chains (illustrated with dotted circle) becomes larger by increasing C, as shown in Figure 8a. At $C \approx C^*$, the envelopes start to overlap each other. However, since

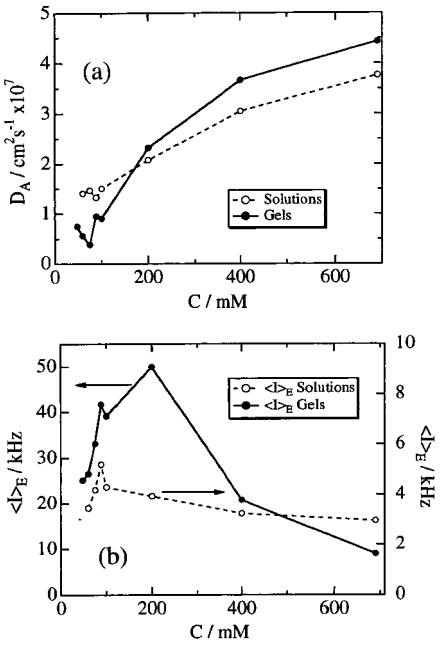

Figure 9. Monomer concentration dependence of the apparent diffusion coefficient, D_A, and ensemble average scattered intensity, $\langle I \rangle_E$.

the monomers on a chain cannot recognize whether they belong to the same chain or not, interchain overlapping takes place without significant potential barrier. Therefore, polymer chains intermix progressively with each other with increasing C. This is why no noticeable broadening is observed in $P(\Gamma^{-1})$. In the case of gels, on the other hand, segregation between monomers belonging to different clusters may be stronger than in the case of polymer solutions due to the presence of cross-links, as shown in Figure 8b. The cross-links prevent mixing of different clusters against thermal fluctuations. Hence, the size of polymer clusters is preserved up to a higher value of C. As a result, a wide distribution of polymer chain clusters is observed, as shown in Figure 5. For $C \geq 200$ mM, a unimodal distribution of $P(\Gamma^{-1})$ is recovered, indicating formation of an infinite network. This argument immediately leads to a conclusion that the gelation threshold can be determined by the characteristic decay time distribution analysis.

Now we discuss the C dependence of the cooperative diffusion coefficient as well as the scattered intensity. Figure 9 shows the variation of (a) D_A and (b) $\langle I \rangle_E$ for gels and polymer solution with C, where $\langle I \rangle_E$ is obtained by taking the ensemble average of $\langle I \rangle_T$. As shown in Figure 9a, D_A is an increasing function of C for both the polymer solutions and gels. Note that D_A for finite cluster solutions is lower than that for linear polymer solutions for $C < 200$ mM. This indicates that the cluster size for the cross-linked system is larger than that of the linear polymer solutions. In the case of the cross-linked system with $C \geq 200$ mM, D_A is estimated by taking account of the nonergodic nature of gels.[13] In this concentration regime, i.e., $C > C^*$, the obtained values of D_A for gels are larger than D_A for polymer solutions. This result is in good agreement with that of our previous work on the cross-link density dependence of the cooperative diffusion coefficient.[21]

Several interesting facts can be obtained from Figure 9b. (1) The scattered intensity from cross-linked polymer chains in a solvent is much stronger than the linear polymer chain in a solvent at a given concentration, indicating larger concentration fluctuations in the former. This is in accordance with the results about the effect of cross-links on scattered intensity reported in the literature.[21,22] (2) $\langle I \rangle_E$ has a maximum around $C = 100$ mM, which is close to C^*. (3) In the case of a cross-linked system, C^* is shifted to a higher concentration because of the exclusive nature of cross-linked polymer chains. (4) For $C \gg C^*$, the scattered intensity decreases with C because concentration fluctuations are suppressed with C. This is again in good agreement with the one in our previous work.[16] Therefore, it is clear that the similarity and dissimilarity between two systems can be elucidated by monitoring D_A and $\langle I \rangle_E$ as a function of C.

4. q Dependence of $P(\Gamma^{-1})$. In order to clarify the nature of the characteristic decay time, Γ^{-1}, the q dependence of $P(\Gamma^{-1})$ was examined. Figure 10 shows $P(\Gamma^{-1})$ vs $q^2\Gamma^{-1}$ plots for NIPA gels, where $P(\Gamma^{-1})$ was obtained at the scattering angle θ of 90° ($q = 0.0187$ nm^{-1}), 75° ($q = 0.0161$ nm^{-1}), 60° ($q = 0.0132$ nm^{-1}),

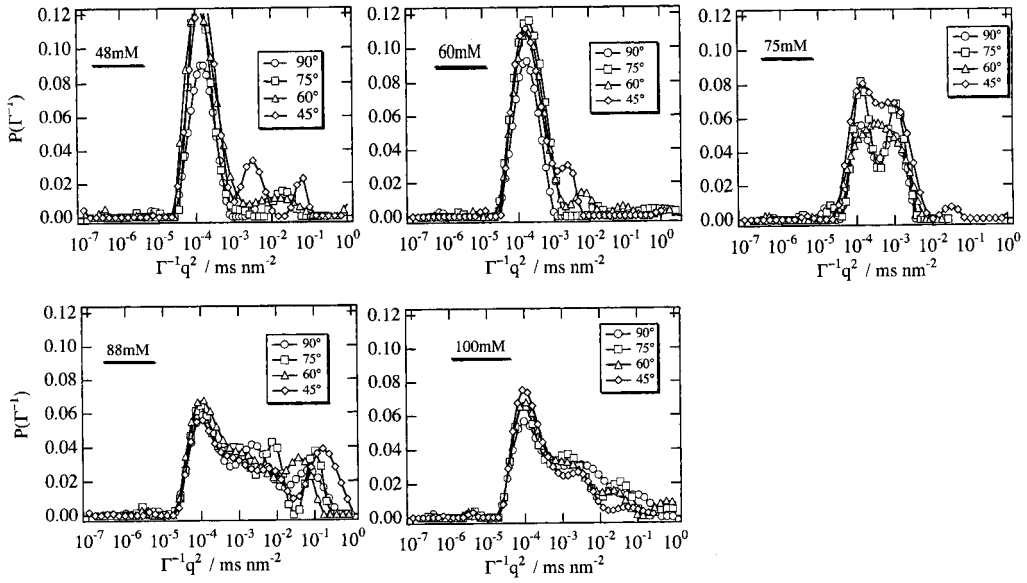

Figure 10. $P(\Gamma^{-1})$ vs $q^2\Gamma^{-1}$ plots for cross-linked polymer chains and linear polymer chains in a solvent.

and 45° ($q = 0.0101$ nm^{-1}). Interestingly, all of the distribution functions at a given monomer concentration are roughly superimposed to a single distribution function, although some deviations are seen. This fact suggests that not only the "small-cluster mode dynamics" represented by the strong peak around 10^{-4} ms nm^{-2} (for $C \leq 60$ mM) but also the "large-cluster-mode dynamics" characterized by a broad tail (for $C = 75-100$ mM) is diffusive mode. The "gel mode" for $C \geq 200$ mM is also diffusive. Therefore, it is concluded that all of the polymer chain dynamics studied in this work are classified to be a diffusive mode. It is needless to mention that a such diffusive mode is also observed for NIPA polymer solutions.

Conclusion

The dynamics of cross-linked NIPA polymers chains in a solvent was investigated by dynamic light scattering. The observed characteristic decay time distribution function, $P(\Gamma^{-1})$, shows three characteristic features, depending on the monomer concentration, C. For $C \leq 60$ mM, $P(\Gamma^{-1})$ has a single peak, corresponding to the cluster size of individual polymers (the small-cluster mode). However, $P(\Gamma^{-1})$ is highly broadened to the large Γ^{-1} side when C is close to the chain overlap concentration for $88 \leq C \leq 100$ mM (the large-cluster mode). This broadened $P(\Gamma^{-1})$ becomes narrow and unimodal by further increasing C ($\geq$200 mM). This corresponds to the so-called gel mode scattering. All of the three modes are confirmed to be diffusive. Therefore, it is demonstrated that $P(\Gamma^{-1})$ is a sensitive measure for the detection of the gelation threshold, and the gel mode scattering is represented by a single exponential function. On the other hand, such broadening in $P(\Gamma^{-1})$ was not observed for NIPA linear polymer solutions. This is a strong indication that linear polymer chains in a solvent near C^* are easier to interpenetrate to each other than the cross-linked polymer chains at the same concentration.

Acknowledgment. This work is partially supported by the Ministry of Education, Science, Sports, and Culture, Japan (Grant-in-Aid, 09450362 and 10875199 to M.S.). The authors are grateful to the helpful comments by Y. Shiwa, Kyoto Institute of Technology.

References and Notes

(1) Martin, J. E.; Wilcoxon, J. *Phys. Rev. Lett.* **1988**, *61*, 373.
(2) Martin, J. E.; Wilcoxon, J.; Odinek, J. *Phys. Rev. A* **1991**, *43*, 858.
(3) Tanaka, T.; Hocker, L. O.; Benedek, G. B. *J. Chem. Phys.* **1973**, *59*, 5151.
(4) Munch, J. P.; Ankrim, M.; Hild, G.; Candau, S. *J. Phys. Lett. (Fr.)* **1983**, *44*, L-73.
(5) Adam, M.; Delsanti, M.; Munch, J. P.; Durand, D. *Phys. Rev. Lett.* **1988**, *61*, 706.
(6) Martin, J. E.; Wilcoxon, J.; Adolf, D. *Phys. Rev. A* **1987**, *36*, 1803.
(7) Adolf, D.; Martin, J. E.; Wilcoxon, J. *Macromolecules* **1990**, *23*, 527.
(8) Shibayama, M.; Fujikawa, Y.; Nomura, S. *Macromolecules* **1996**, *29*, 6535.
(9) de Gennes, P. G. *Scaling Concepts in Polymer Physics*; Cornell University: Ithaca, NY, 1979.
(10) Provencher, S. W. *Comput. Phys. Commun.* **1982**, *27*, 213.
(11) Provencher, S. W. *Comput. Phys. Commun.* **1982**, *27*, 229.
(12) Chu, B. *Laser Light Scattering*; 2nd ed.; Academic Press: New York, 1991.
(13) Joosten, J. G. H.; McCarthy, J. L.; Pusey, P. N. *Macromolecules* **1991**, *24*, 6690.
(14) Peters, R. In *Dynamic Light Scattering: The Methods and Some Applications*; Brown, W., Ed.; Oxford University Press: Oxford, U.K., 1993.
(15) Pusey, P. N.; van Megen, W. *Physica A* **1989**, *157*, 705.
(16) Norisuye, T.; Shibayama, M.; Nomura, S. *Polymer* **1998**, *39*, 2769.
(17) Panyukov, S.; Rabin, Y. *Phys. Rep.* **1996**, *269*, 1.
(18) Shibayama, M. *Macromol. Chem. Phys.* **1998**, *199*, 1.
(19) Fujita, H. *Polymer solution*; Elsevier: Amsterdam, 1990.
(20) Kubota, K.; Fujishige, S.; Ando, I. *Polym. J.* **1990**, *22*, 15.
(21) Shibayama, M.; Norisuye, T.; Nomura, S. *Macromolecules* **1996**, *29*, 8746.
(22) Mallam, S.; Horkay, F.; Hecht, A. M.; Geissler, E. *Macromolecules* **1989**, *22*, 3356.

MA9801826